

Experimental study on flexural strength of reinforced modular composite profiled beams

Hyung-Joon Ahn

Department of Architectural Engineering, Kon-Kuk University, Seoul, Korea

Soo-Hyun Ryu[†]

Department of Architectural Design, Sahm-Yook University, Seoul, Korea

(Received October 5, 2007. Accepted June 1, 2008)

Abstract This study attempts to suggest bending reinforcement method by applying bending reinforcement to composite profile beam in which the concept of prefabrication is introduced. Profile use can be in place of framework and is effective in improvement of shear and bending strength and advantageous in long-term deflection. As a result of experiment, MPB-CB2 with improved module had higher strength and ductility than the previously published MPB-CB and MPB-LB. In case of bending reinforcement with deformed bar and built-up T-shape section based on MPB-CB2, the MPB-RB series reinforced with deformed bar were found to have higher initial stiffness, bending strength and ductility than the MPB-RT series. The less reinforcement effect of the MPB-RT series might be caused by poor concrete filling at the bottom of the built-up T-shape. In comparison between theoretical values and experimental values using minimum yield strength, the ratio between experimental value and theoretical value was shown to be 0.9 or higher except for MPB-RB16 and MPB-RT16 that have more reinforcement compared to the section, thus it is deemed that the reinforced modular composite profiled beam is highly applicable on the basis of minimum yield strength.

Keywords : modular; composite profiled; flexural strength; bending reinforcement; prefabrication.

1. Introduction

In addition to the reinforcing bar, each type of reinforcement has been studied to increase the strength and ductility of RC beams. Among these types of reinforcement, profile has been formerly used as a deck plate in a slab, and studies extending this profile concept to a beam started in Australia in 1990s. Existing methods include the joining of a side plate onto the constructed RC beam with a bolt(Oehlers *et al.* 1997, 2000) or adhesive(Oehlers *et al.* 2000) and reinforcement with FRP(Minglan *et al.* 2004) and CFRP(Kim *et al.* 2004). As an existing study about composite profile beams, Oehlers(1993) performed a comparative study on the bending and shear strength of a side profiled beam and a reinforced concrete beam, and suggested an equation to calculate the flexural strength of profiled beams based on the shear connection ratio under the rigid plastic analysis theory.(Oehlers *et al.* 1994) Brian Uy *et al.* compared experimental moment-curvature feature of a composite profile beam and a reinforced concrete beam with

[†]Assistant Professor, Corresponding author, Email : ryu129@hanmail.net

these features to those obtained from a theoretical equation incorporating the slip strain parameter. (1995) Also, numerical analysis with variables of each kind was conducted by applying a theoretical equation. (Brian Uy *et al.* 1995) The author suggested the side and lower modules of C-Type and Lip-Type in a previous study (Ahn *et al.* 2007), and conducted the analytical study with the parameters of bolt connection and tension plate reinforcement. Thus, the present study is carried out under the following three differentiated points based on previous studies: First, the concept of permanent profile formwork as a substitute for the existing temporary formwork was introduced; this profile could greatly contribute to improved bending and shear resistance as well as function of temporary formwork and enhance the displacement of beams. Second, the existing SC beam was made at the shop once the necessary size was ordered and then used in the construction field, but the concept of modules was introduced into the profile beam, which enabled free molding of a member of a desired size once simplified module was assembled. Third, bending strength was secured by reinforcement of a corresponding amount onto a necessary part. Based on this concept, in this study, a module of the improved version of the published Modular composite Profiled Beams (hereafter MPB) was developed and the applicability was proven. An MPB was reinforced to obtain the necessary bending strength based on the improved module, and a comparative analysis on the bending behavior between rigid plastic analysis theory and experimental result was carried out. With these efforts, this study attempts to verify the applicability of the Reinforced Module Type Composite Profile Beam (hereafter MPB-R) through measurement and analysis of the behavioral characteristics for each part such as the slip between modules etc.

2. Flexural Strength of MPB-R

The reinforced MPB was analyzed by reference to the equation suggested by Oehlers's theoretical method (1993, 1994). The section shape of the profile beam used in experiment and analysis is shown in Fig. 1. MPB-CB2 is a specimen with improved bottom module of MPB-CB which was used in a previously published study (Ahn *et al.* 2007). MPB-RT is a specimen reinforced with welded T-type section and MPB-RB is a specimen reinforced with deformed bar, and strength by reinforcement is indicated as P_r in a theoretical equation.

Fig. 2 (a) shows each module of Fig. 1(a) specimen and Fig. 2(b) shows each module of Fig. 1(b), (c) and (d) specimens.

Section area and the details of T-type and bar reinforcement are as mentioned in Table 1.

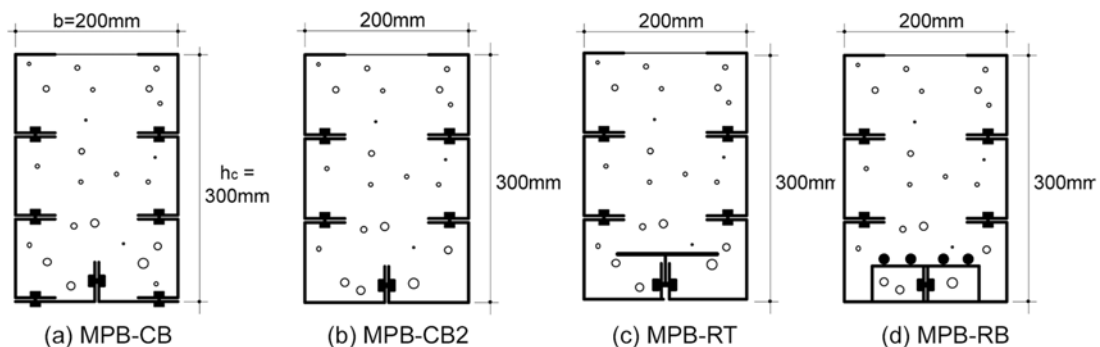


Fig. 1 Shape of Specimen Section

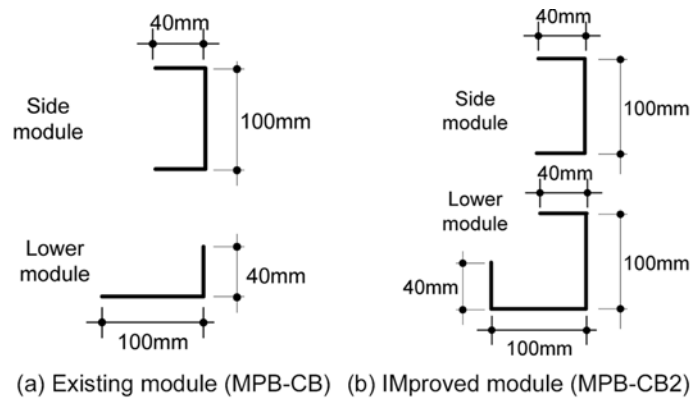


Fig. 2 Comparison between Modules

Table 1 Detail of Reinforced Modules

Specimens	T-type B × H × t1 × t2(mm) or Deformed Bar	Section Area of Reinforcement	Reinforcement Section
MPB- CB2	-	-	-
MPB-RT10	65 × 25 × 3.2 × 3.2	288 mm ²	
MPB-RT13	65 × 25 × 6.0 × 5.0	515 mm ²	
MPB-RT16	65 × 32 × 9.0 × 6.0	777 mm ²	
MPB-RB10	4-D10	284 mm ²	
MPB-RB13	4-D13	508 mm ²	
MPB-RB16	4-D16	796 mm ²	

2.1 If slip does not occur in each module

Fig. 3 shows behavior of the concrete elements. If a reinforced concrete element is bent and compressed, the concrete element and bond stress will result in a compressive element and a tension element, respectively and cause a moment. Considering the equilibrium of force, compressive stress and tension stress by reinforcement of concrete are described in the following equation:

$$C_c = 0.85f_{ck}\beta_1N_c b = P_r + P_b \tag{1}$$

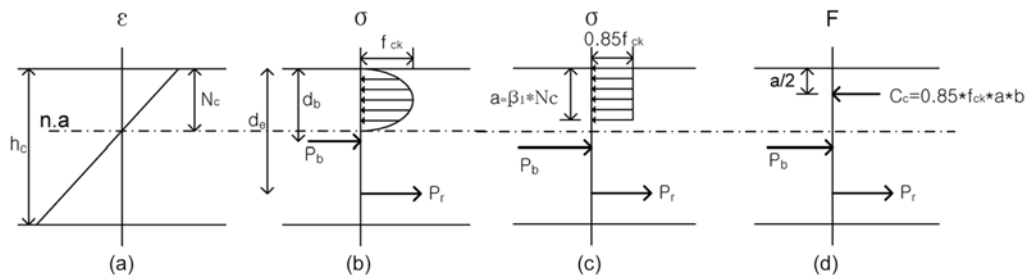


Fig. 3 Behavior of Reinforced Concrete Elements

Here, C_c is compressive stress of the concrete, P_b bond stress of the profile and concrete, and P_r tension stress of the reinforcing member. The neutral axis N_c is summarized:

$$N_c = \frac{P_r + P_b}{0.85f_{ck}\beta_1 b} \quad (2)$$

Fig. 4 shows behavior of the profile elements, and N_p indicates the neutral axis. The general equilibrium of the forces of concrete and profile can be obtained only on condition that bond stress acting toward the tension direction of concrete works in the compressive direction in the profile. Thus, the equilibrium of force can be indicated in the equation:

$$P_c + P_b = P_t \quad (3)$$

Here, P_c = compressive stress of the profile in the compressive part

P_t = tension stress of the profile in the tension part

Fig. 4(c) is the strain of Fig. 4(b) by the addition of compressive stress and f_y of the tension stress to the compressive direction of the profile, where there is no change in the equilibrium of the force. When Eq. (3) applies to the transformed stress distribution as shown in Fig. 4(c), the following equation is obtained:

$$f_y t_e (2h_c + b) = 2 \times 2f_y t_e N_p + P_b \quad (4)$$

Here t_e is effective thickness and indicated in $t_e = \frac{St}{2h_c + b}$ by reference to Fig. 1, and S is the whole length of profile and t is the thickness of profile.

Eq. (4) for the neutral axis N_p of the profile is summarized:

$$N_p = \frac{f_y t_e (2h_c + b) - P_b}{4f_y t_e} \quad (5)$$

The moment capacity of MPB-R is M_p , which can be obtained by taking the bending moment of the upper end of the section, as shown in Fig. 1(d) and Fig. 2(d); the contribution of the bond force to the moment capacity is zero because it acts in opposite directions and at the same location on the two sections.

$$M_p = f_y t_e (h_c^2 + bh_c - 2N_p^2) + P_r \times d_e - \frac{0.85f_{ck}a^2 b}{2} \quad (6)$$

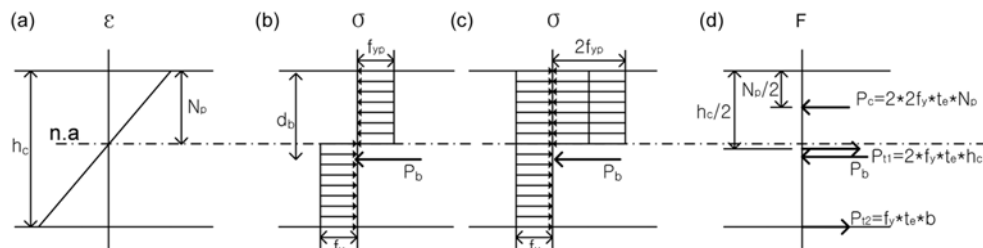


Fig. 4 Behavior of Profile Elements

2.1.1 Full shear connection

Upon full shear connection, slip is 0, resulting in $N_c = M_p$. Therefore, $(P_b)_{fsc}$, required to get the full shear connection, is obtained through the equipollence of Eq. (2) and Eq. (5):

$$(P_b)_{fsc} = \frac{f_y t_e (2h_c + b) \times 0.85 f_{ck} \beta_1 b - 4t_e f_y P_r}{4f_y t_e + 0.85 f_{ck} \beta_1 b} \quad (7)$$

Bending moment (M_p) upon full shear connection can be obtained by inserting $(P_b)_{fsc}$ from Eq. (7) into Eq. (2) and Eq. (5) to get N_c and N_p , and then applying this result to Eq. (6).

2.1.2 Partial shear connection

Each value of N_c and N_p is obtained by changing $(P_b)_{psc}$ into according to the degree of shear connection to get bending moment by substituting these for Eq. (6). For example, if a shear connection

ratio is 50%, $(P_b)_{psc} = 0.5 \times (P_b)_{fsc}$. Here shear connection ratio is $\frac{(P_b)_{psc}}{(P_b)_{fsc}}$.

2.1.3. No shear connection

There is no shear connection when $P_b = 0$, and $N_c = \frac{P_r}{0.85 f_{ck} \beta_1 b}$ in Eq. (2) and $N_p = \frac{f_y t_e (2h_c + b)}{4f_y t_e}$ in Eq. (5). Bending moment exercises individual strength by separation of concrete and profile.

2.2 Slip occurrence between modules

2.2.1. Partial shear connection (psc)

If slip occurs between modules of MPB, strain incurred to profile and concrete is as shown in Fig. 5(b) and Fig. 5(e) and strength in Fig. 5(c) and (f). In this case, bending moment (M_p) is obtained by putting the bending moment toward the top by stress equivalent to a non-slipped amount of profile, the moment toward the top of reinforced concrete, and the moment of individual profile equivalent to a slipped amount together.

$$(M_p)_{psc} = P'_{(3)}(h_c - h_3) + P'_{(2)}(h_c - 1.5h_m) - P'_{(1)}(h_c - 2.5h_m) + P_r \times d_e - C_c \frac{a}{2} + \sum M_m \quad (8)$$

Here $P_{(a)}$: tension force of steel sheet in non-slip portion

h_c : height of specimen

h_m : height of each module

M_m : bending moment of each module in portion of slip ratio

C_c : compression force of concrete in the case of full shear connection

P_r : Tension force of the reinforcing member

d_e : Distance from center of the reinforcing member to the edge of compression

h_3 : Center of figure for the No.3 module

For instance, if the slip ratio is 30%, 70% of the tension stress of each profile contributes to bending of the total section, resulting in $P_{(a)}$, and the slipped 30% contributes to M_m of the individual profile.

2.2.2. No shear connection (nsc)

$(M_p)_{nsc}$, without bond stress of concrete and profile for MPB-R, is the sum of the bending moment of

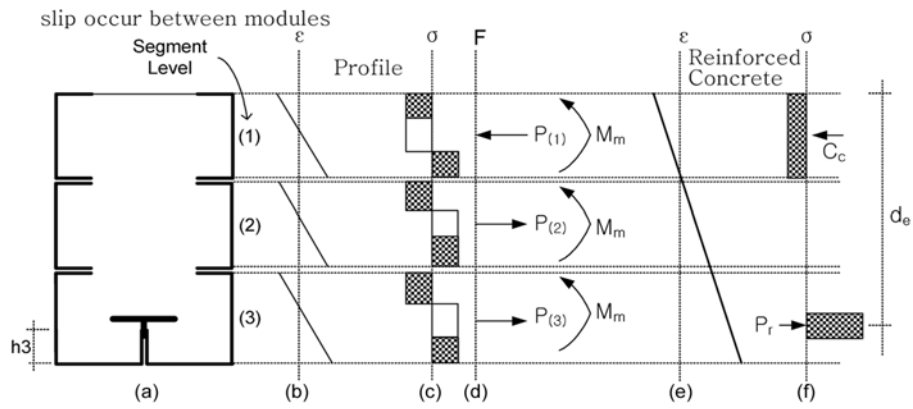


Fig. 5 Distribution of Stress and Strain by Slip between Modules

each module and those of the internal reinforcing element and concrete.

3. Test Setup

3.1 Test specimens

In this experiment, for tension reinforcement, reinforcing capacity was evaluated for the two cases of bar and plate. A total of seven specimens were prepared for this experiment: MPB-RB10 specimen reinforced

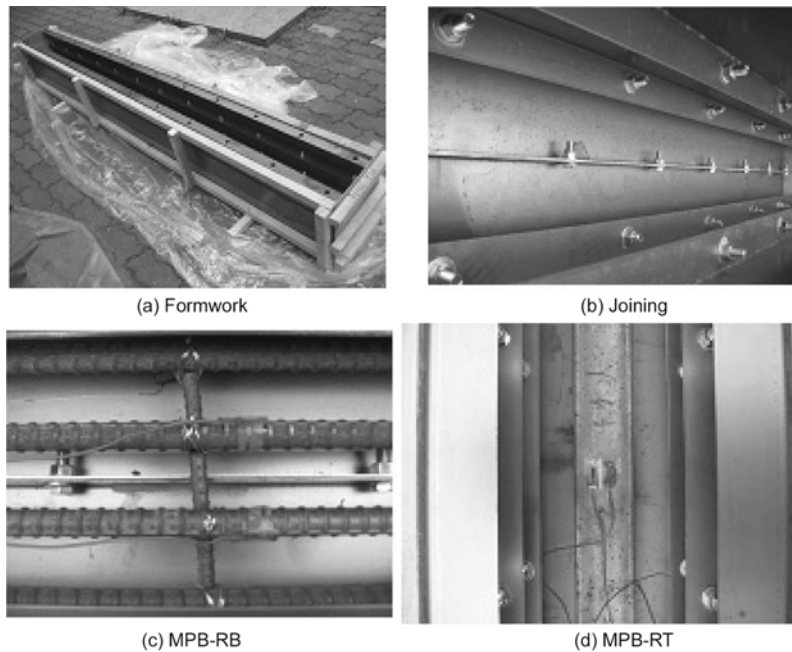


Fig. 6 Specimen Made

with 4 deformed bars of 10 mm, MPB-RB13 specimen reinforced with 4 deformed bars of 13 mm, MPB-RB16 specimen reinforced with 4 deformed bars of 16 mm; MPB-RT10 specimen reinforced with a plate having a similar section area to B10, MPB-RT13 specimen having similar section area to B13, and MPB-RT16 specimen having similar section area to B16; and CB2 specimen without reinforcement. Connection methods of modules are by arrangement of general bolts of 8 mm in diameter and 25 mm in length at intervals of 200 mm. For the improved CB2 specimen, performance enhancement was evaluated by comparison with the performance of the existing CB specimen, and comparative analysis on the reinforced specimens was carried out between theoretical result and experimental result to determine the improvement in stiffness and strength according to the amount of reinforcement.

3.2 Experiments of material

3.2.1 Experiment of concrete compression strength

The concrete used in this specimen had 24 MPa of specified compressive strength and was cured after casting in place. The specimen made under KS F 2403 was cured under the same conditions as the experiment, and compressive strength of the concrete cylinder at 28 days was found to be about 26 MPa.

3.2.2 Experiment of tensile strength of profile

The specimen used in this experiment was SS400, the rolled plate of KS D 3503. Two specimens were made by thickness and diameters.

3.3 Loading and measurement

For loading of the specimen, 2-point loading was conducted with a 490 kN universal tester, as shown in Fig. 7. Two LVDTs were placed at the left and right sides in the center of the beam for measurement of displacement. A strain gauge for steel was attached to the top, middle and bottom of the side module and the top and bottom of the beam. A concrete gauge was attached to the top of the center of the beam to examine the behavior of concrete in the compression direction.

4. Experimental Result

4.1 Destruction shape

4.1.1 MPB-RB & MPB-CB2

Fig. 8 shows the failure shape of MPB-RB & MPB-CB2. With increased strain after maximum load, local buckling occurred at the bottom steel with a loading point, significant separation between modules occurred at the bottom of local buckling with increased deflection, and the side steel failed with lateral

Table 2 Concrete Mixing Ratio

Design Strength (MPa)	W/C(%)	Slump(mm)	Unit of Aggregate (kg/m ³)			
			W	C	S	G
24	50.4	145	177	353	843	943

W : Water, C : Cement, S : Fine Aggregate, G : Coarse Aggregate

Table 3 Test Results of Sheet & Plate & Deformed Bar

Specimen	f_y	f_u	E	ϵ_y	f_y/f_u	Elongation Ratio(%)
1.6 mm	372.40	423	204100	1830	0.88	27
3.2 × 25	323.40	495.88	177234	1834	0.65	21
5 × 25	351.82	503.05	186740	1884	0.70	22
6 × 65	357.00	512.30	199047	1717	0.70	22
9 × 65	326.34	484.60	159881	1546	0.67	23
D10	541.94	691.52	187807	2914	0.59	20
D13	405.72	594.94	173342	2374	0.68	22
D16	496.86	616.07	217354	2614	0.81	17

f_y : Yielding Strength(MPa), f_u : Tensile Strength(MPa), E : Young's Modulus(MPa), ϵ_y : Yielding Strain($\times 10^{-6}$), f_y/f_u : Yielding Ratio

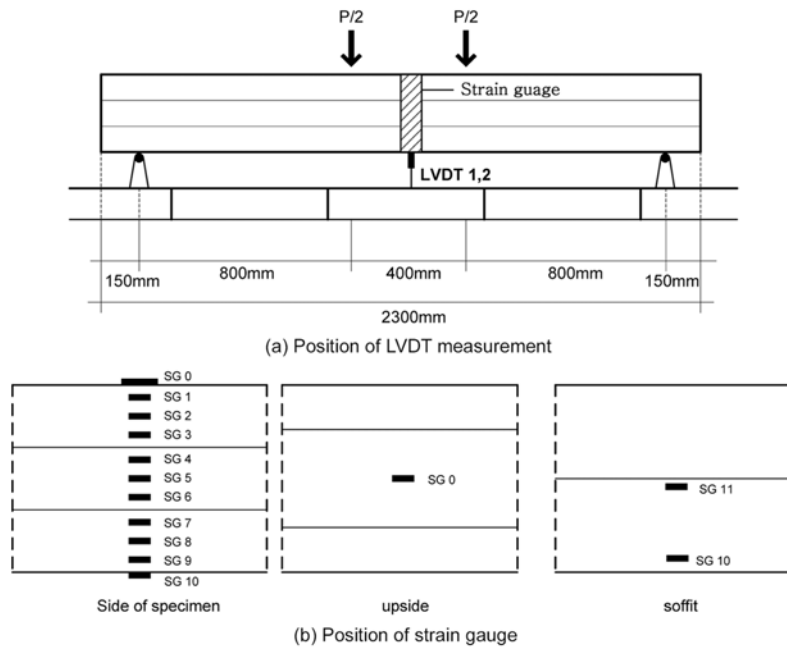


Fig. 7 Measurement Position and Strain Gauge Attachment Position

buckling as shown in Fig. 8(f). Contrary to CB2, the MPB-RB series specimens had crack at the caps on both ends upon failure, which indicates that the internal deformed bar delivered enough strength to concrete.

4.1.2 MPB-RT

Fig. 9 is the failure shape of MPB-RT. With compressive failure of concrete before maximum load, local buckling occurred in the steel around the loading point, and the steel failed with increased deflection and sudden separation between modules. Contrary to the MPB-RB series, a little crack at the caps on both ends occurred in T10 but no crack occurred in the others because the T-type section of reinforcement might not display enough stress.

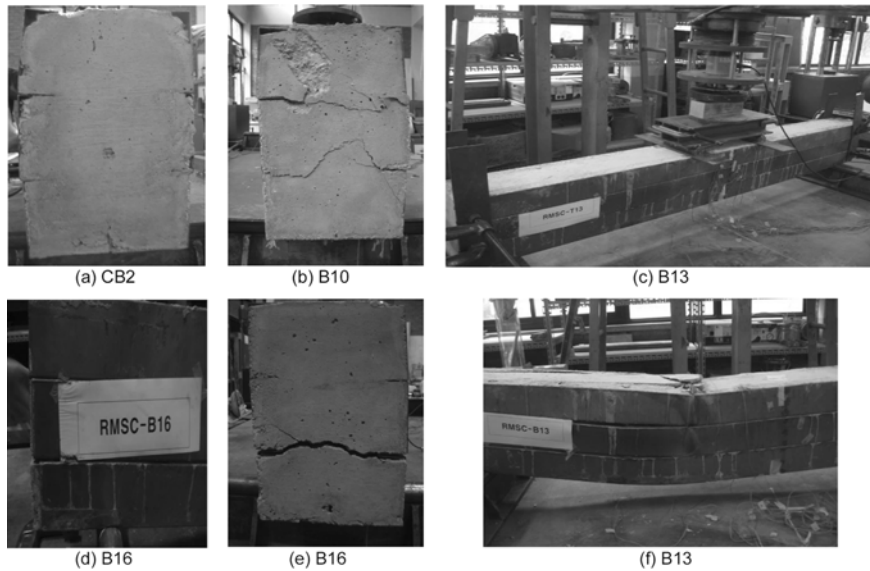


Fig. 8 Failure Shape of MPB-RB & MPB-CB2

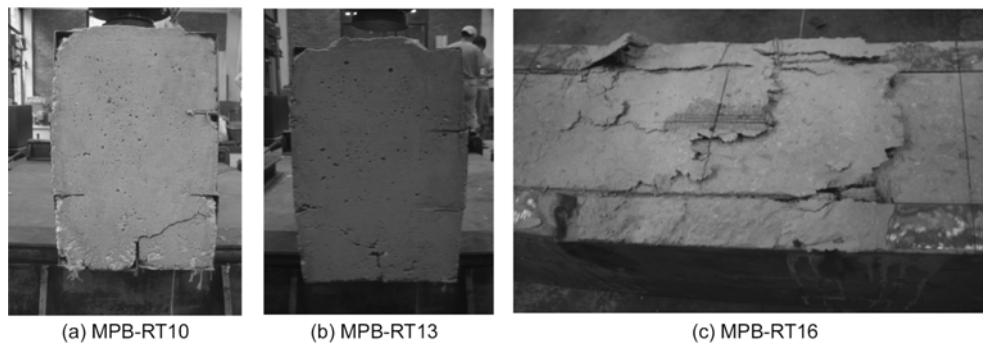


Fig. 9 Failure Shape of MPB-RT

4.2 Load-displacement and load-strain curves

4.2.1 Load-center displacement

Fig. 10 shows the comparison of load-displacement curves among the specimens. Most specimens showed sufficient displacement ability. The MPB-RT series reinforced specimens showed lower maximum strength than the non-reinforced specimens despite their plate reinforcement, and the MPB-RB series specimens reinforced with bar showed greater maximum strength than the non-reinforced specimens. Of the MPB-RB series, specimens B10 and B13 did not reach plastic plateau after maximum load and only showed a sharply decreased load. The strength of the MPB-RT series was reduced mostly by poor concrete filling at the bottom of the T-type and slip between plate and concrete.

4.2.2 Load-strain curve of top fiber concrete

Fig. 11 shows the load-strain curves of the upper concrete. The MPB-CB2 specimen shows an

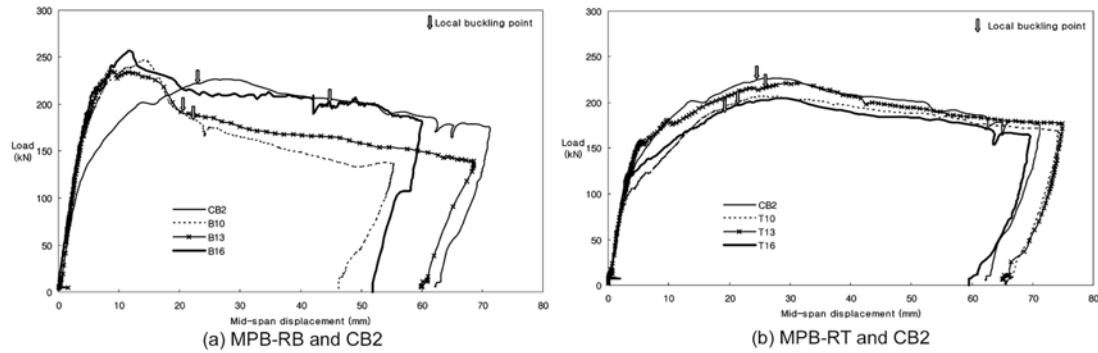


Fig. 10 Load-center Displacement

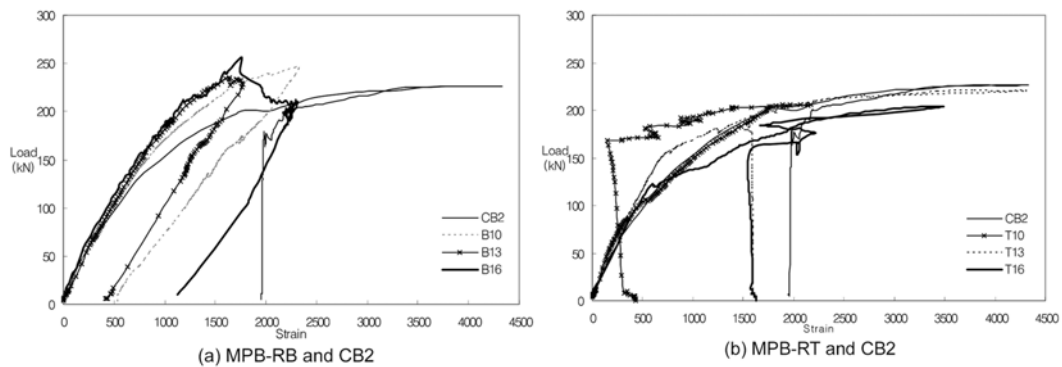


Fig. 11 Concrete Strain

increase in concrete strain with increase in load, which amounts to 6000 in concrete strain; thus, it is considered that the concrete fully contributed to the increase in strength.

The MPB-RT series specimens show the pattern of compression failure due to a sharp increase of strain under maximum load, while the MPB-RB series specimens neither show a sharp increase of strain nor exceed the maximum strain measured in experiments of material, indicating that the MPB-RT series gave greater displacement under maximum load.

4.2.3 Load-strain curve of bottom-fiber steel

Fig. 12 shows the load strain curves of the bottom members. The MPB-RT series including MPB-CB2 showed large strain because of the greater strain with increase of load, and the lower module greatly influenced the bending behavior. On the contrary, MPB-RB series specimens did not exceed yield strain until the end of the experiment.

4.2.4 Load-strain curve of reinforcement element

Fig. 13 shows the load-strain curves of the reinforcing member in concrete. For the MPB-RT series, strain was measured by attachment of the strain gauge to the upper part of the T-type reinforcement, and the MPB-RT10 specimen gauge was early missed. The MPB-RT series showed tension through behavior in a body with concrete at the early stage and compression through separation from concrete by slip.

The MPB-RT16 specimen showed compression yielding by full separation of the reinforcing member

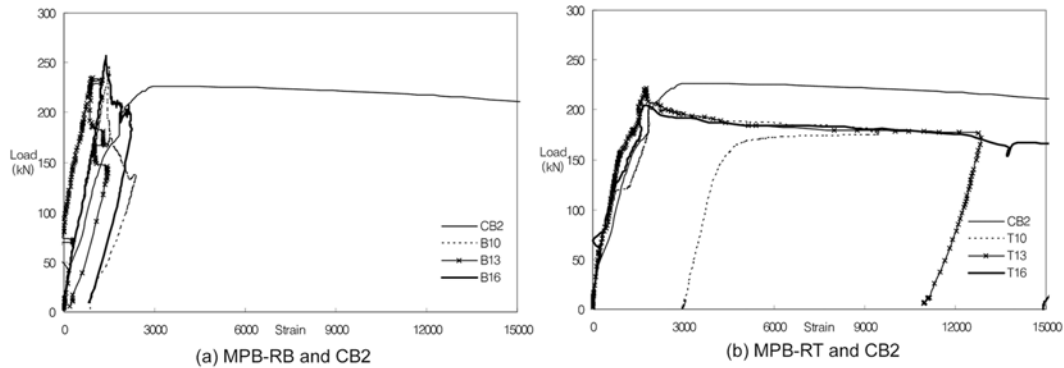


Fig. 12 Load-strain Curve of Bottom-fiber Steel

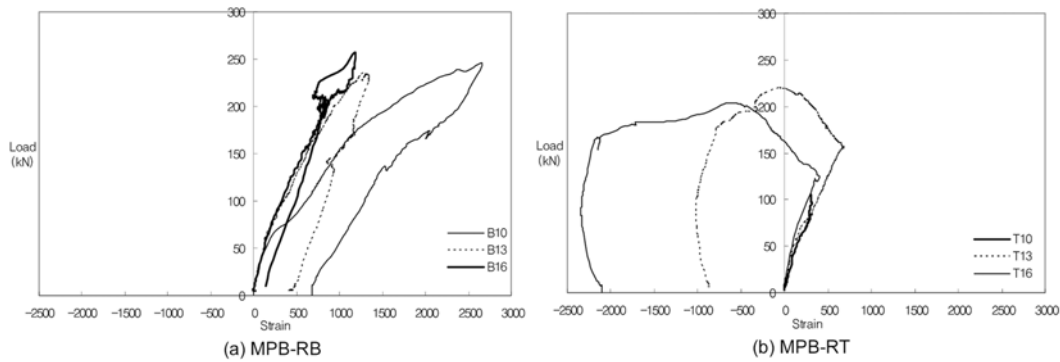


Fig. 13 Load-strain Curve of reinforcement element

from the concrete after maximum load. In the MPB-RB series, the B10 specimen showed the greatest strain and reached yielding, and B13 and B16 showed strain equivalent to about half the yielding strain. Consequently, the B10 specimen, whose reinforcing member yielded, showed the maximum strength, which most closely approximated the theoretical value.

4.3 Analysis and discussion

4.3.1 Analysis on bending strength

1) Comparison between CB2 and the published profile beam by Ahn *et al.* (2007)

Fig. 14 shows the shape of the published section, and Table 4 shows the theoretical and experimental maximum loads and the initial stiffness section ratio of the improved CB2 and the published module profile beam(MPB-CB , MPB-LB) specimens. The section area ratio is the value that the section area of each specimen is divided by that of the CB2 specimen of base. The load ratio of CB2 is 0.84, which is higher than 0.76 of CB and 0.8 of LB, and approximates 0.88 of the uneven section of the single section. The initial stiffness shows a similar pattern to that of the published specimen.

Fig. 15 shows that the improved CB2 specimen has enough ductility and that the fully plastic plateau appears after the maximum load. Thus, it is considered that the CB2 specimen has better bending behavior than both the LB specimen, which has a great stiffness but a sharply decreased load after the maximum load, and the CB specimen, which does not fully display strength.

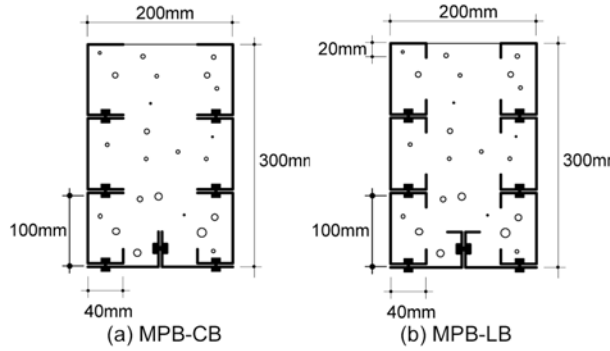


Fig. 14 Section Shape Published

Table 4 Comparative Analysis between Experimental Result and Theoretical Analysis

Specimen	Theory(kN) P'_{max}	Experiment(kN) P_{max}	Initial Stiffness	Section Area Ratio
			$\frac{P_y}{\delta_y}$	$\frac{A}{A_{CB2}}$
MPB-CB2	271.23	226.48	20.02	1
MPB-CB	281.03	213.31	21.79	1.06
MPB-LB	327.80	263.29	36.09	1.28

2) Analysis of MPB-RT

Table 5 shows the comparison between theoretical and experimental maximum loads. The theoretical maximum load was calculated based on the assumption that the modules were fully interconnected and the profile and concrete were fully connected. For the CB2 specimen, P_{me} / P_{mt} value is 0.84. When CB2 is analyzed with the theoretical equation developed in Section 2, the maximum strength is 271 kN upon full bond without slip, 240 kN upon 50% bond without slip, and 224 kN upon 20% slip, where the experimental value 226 kN is similar to the theoretical value for lowered bond stress without slip between the modules. Also, slip occurred as shown by the changes in the strain of side profile in Fig. 18(a), where the theory of Section 2.2.1 could be applied. Here, the slip ratio is the ratio of the profile

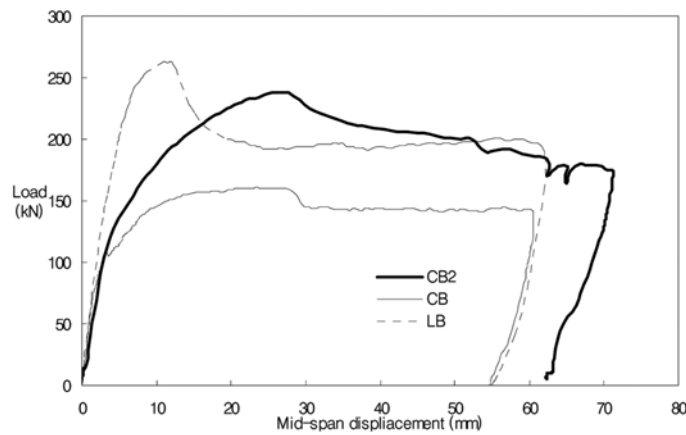


Fig. 15 Comparison of Central Load-Displacement between MPB-CB2 and published MPB

Table 5 Comparative Analysis of Maximum Load on MPB-RT

Specimen	Theory(kN) P_{mt}	Experiment (kN) P_{me}	$\frac{P_{me}}{P_{mt}}$	Theory(kN) P_{mt2}	$\frac{P_{me}}{P_{mt2}}$
MPB-CB2	271.23	226.48	0.84	181.00	1.25
MPB-RT10	311.73	206.05	0.66	211.15	0.98
MPB-RT13	336.45	222.25	0.66	232.68	0.96
MPB-RT16	356.75	204.11	0.57	258.13	0.79

strength to be distributed by bending of individual profiles through slip.

For the MPB-RT series specimens experimental values are lower than theoretical value. This result is mainly caused by the bond that is missing between the reinforcing member and the concrete and by the poor concrete filling at the bottom of the T-type reinforcing member. Therefore, the T-type reinforcing section showed poor reinforcing performance against bending.

The theoretical strength of the specimen was replaced by the minimum yield stress f_y instead of the test result of material property to calculate P_{mt2} and compare it with the experimental value, and the comparison data are as shown in Table 4. Here, the plate is SS400 and $f_y = 235$ MPa, and the bar is SD400 and $f_y = 400$ MPa. Compare result indicates that the experimental values approximated the theoretical values except for T16.

3) Analysis of MPB-RB

The comparison of the maximum bending moment between the theoretical values and the experimental values is as shown in Table 6. The B10 specimen gave the best bending moment among the reinforced specimens, where P_{me}/P_{mt} value was 0.75. From the results of analysis with the theoretical equation developed in Section 2, maximum strength was found to be 327 kN upon full bond without slip, 309 kN upon 50% bond without slip, and 243 kN upon 35% slip, which indicates that the experimental value of 246 kN was similar to the theoretical value upon slip between the modules with lowered bond stress. Also, slip occurred as shown by the changes in strain of the side profile in Fig. 18(d), where the theory of Section 2.2.1 could be applied. Except the B10 specimen, B13 and B16 specimens showed low ratios of experimental value to theoretical value of 0.68 and 0.63, respectively, which implies that the strength was not improved due to poor concrete filling and insufficient area of coated concrete by influence of the curtailed experiment. If the compression strength is improved by slab reinforcement in the compression direction and the concept of the T beam is introduced to inhibit profile in the compression direction from the lateral buckling status, better MPB can be developed.

The ratio between experimental value P_{mt2} and theoretical value P_{me} was 1.07 for B10, 0.90 for B13, and 0.84 for B16. Among reinforced specimens, only B10 exceeded a value of 1

Table 6 Comparative Analysis of Maximum Load on MPB-RB

Specimen	Theory(kN) P_{mt}	Experiment(kN) P_{me}	$\frac{P_{me}}{P_{mt}}$	Theory(kN) P_{mt2}	$\frac{P_{me}}{P_{mt2}}$
MPB-CB2	271.23	226.48	0.84	181.00	1.25
MPB-RB10	327.26	246.16	0.75	230.80	1.07
MPB-RB13	345.48	236.13	0.68	266.83	0.90
MPB-RB16	404.63	256.51	0.63	304.55	0.84

4.3.2 Initial stiffness

Initial stiffness by specimen was calculated as shown in Table 7. Initial stiffness was defined as the ratio of yielding load to maximum load; the yielding displacement as the point where the maximum strength and the stiffness of 60% of the maximum strength are connected and met; and the strength as the yielding strength. MPB-RT series specimens showed similar stiffness to CB2, and the reinforcing section did not influence the increase of stiffness. On the contrary, the MPB-RB series specimens displayed greater stiffness than the MPB-RT series and CB2, indicating that the reinforcing effect of the reinforcement member influenced the stiffness. Especially, the initial stiffness of T10 was least as 18.9, which implies that the concrete was not tightly filled at the bottom of T-type reinforcement.

4.3.3 Analysis on strain by position of the strain gauge for each specimen

Fig. 16 shows the distribution of load strain for the side module. No. 1~9 on the vertical axis indicates the positions of the strain gauges, which are shown in Fig. 7, and the horizontal axis indicates the strain. Load is divided into 4 steps, and the distribution of strain by gauge position at each load step is shown. Load step 1 indicates 20% of the maximum load; step 2 50%; step 3 80%; and step 4 the strain of the maximum load. For better understanding of the distribution of strain by experimental step, the values of strain by load step were connected with several lines. No. 1~3 indicate the upper modules, No. 4~6 the central modules, and No. 7~9 the lower modules, respectively.

In all the specimens, a little slip between modules occurred up to 50% of the maximum load of steps 1 and 2, and constant linearity was maintained. The more load there was, the more slip occurred between the modules, and after the maximum load, the separation between the modules became severe. In all the specimens, the side profile showed no fully plastic behavior, indicating that the experimental bending strength could not reach the theoretical value on condition of fully plastic behavior. Regarding CB2, which most closely approximated the fully plastic theoretical value, the side profile contributed to the increase in strength because the strain of the profile in the tension direction exceeded yielding strain under maximum load. For the strain of the compressive side of the MPB-RB series, B10 solely showed yielding strain. For the tension side, the bottom of the lower module of the B16 specimen reached yielding.

Especially, the strain of the tension side of the MPB-RB series tended to be smaller than that of the MPB-RT series owing to influence of the division of strength of the internal bar.

5. Conclusion

From experiments and theoretical analysis on the bending behavior of improved and reinforced MPB,

Table 7 Initial Stiffness and Ductility of MPB-R

Specimen	P_y (kN)	δ_y (mm)	Initial Stiffness $\frac{P_y}{\delta_y}$
MPB-CB2	170.80	8.53	20.02
MPB-RT10	162.40	12.44	13.05
MPB-RT13	163.37	7.40	22.08
MPB-RT16	140.08	7.41	18.90
MPB-RB10	190.86	5.66	33.72
MPB-RB13	191.18	5.17	36.98
MPB-RB16	213.82	6.31	33.89

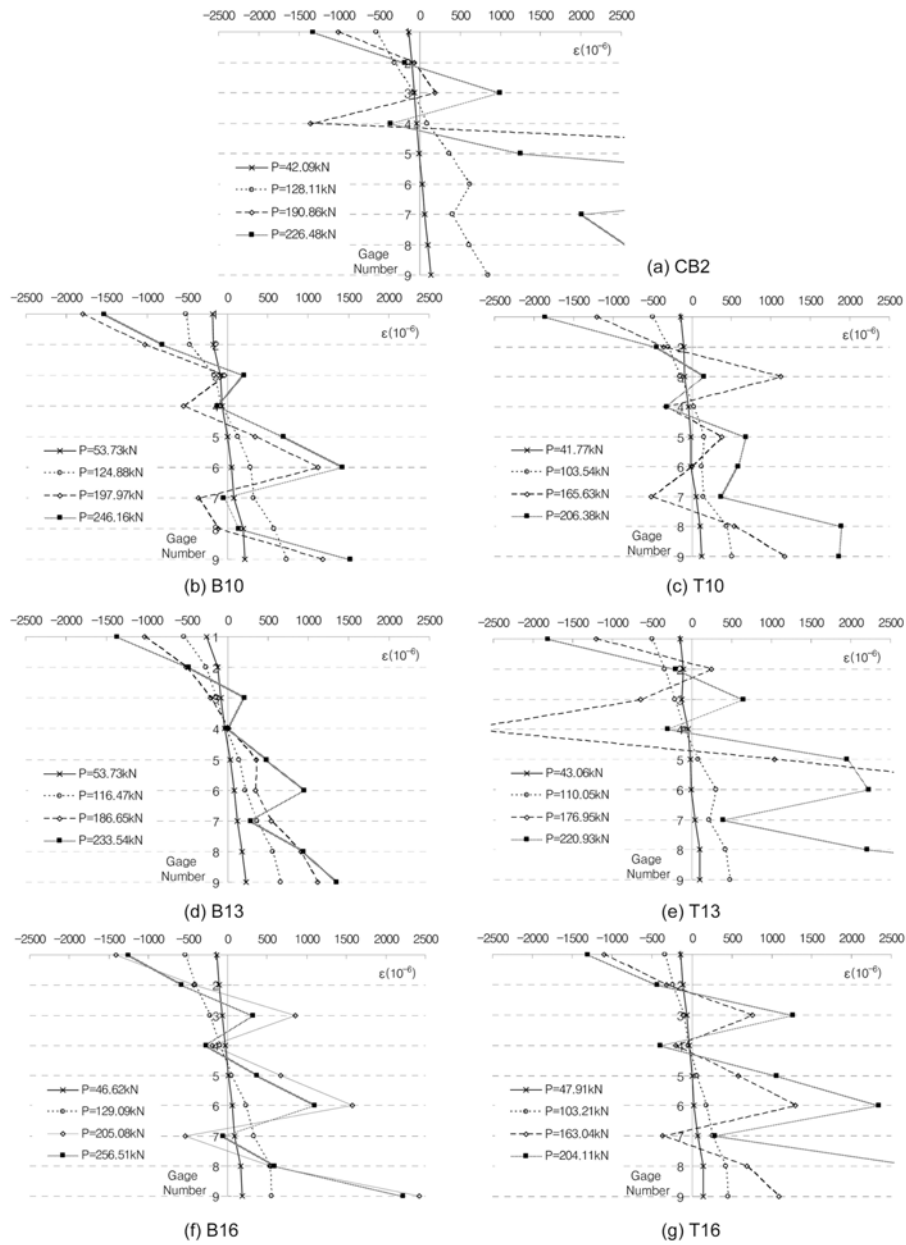


Fig. 16 Distribution of Strain for Side Modules by Specimen

the following conclusion is made:

- For the improved MPB-CB2, a load ratio between experimental value and theoretical value was 0.84, which was higher than 0.76 for the existing MPB-CB and 0.8 for MPB-LB, and sufficient displacement ability and plastic plateau were shown after the maximum load. Therefore, it has a more stable section than the MPB-LB specimen, which has greater stiffness but shows a sharply decreased load after the maximum load, and it displays better bending behavior than the other specimens.

- The MPB-RT series specimens T10, T13, and T16 showed similar stiffness to MPB-CB2, when the reinforced section did not influence the increase in stiffness. However, the MPB-RB series specimens B10, B13, and B16 showed greater stiffness than the MPB-RT series and MPB-CB2, indicating that the reinforcing effect of the reinforcing member influenced the stiffness.
- In all specimens, there was very little slip between the modules up to 50% of the maximum load, and constant linearity was sustained. Thereafter, the more was the load, the more was the slip between the modules, and after the maximum load, and the separation between the modules became severer. No fully plastic behavior of the side profile was shown in all the specimens.
- Regarding the load ratio between experimental value and theoretical value without full bond and no slip, the experimental values were very low as 0.66, for the MPB-RT10, 0.66 for MPB-RT13, 0.57 for MPB-RT16, 0.75 for MPB-RB10, 0.68 for MPB-B13, and 0.63 for MPB-B16. The strength was not improved because of poor concrete filling and insufficient area of coated concrete. Using the minimum yield stress f_y , load ratio exceeded 0.9 in all specimens except for MPB-T16 and MPB-B16. The reinforced MPB is applicable to the minimum yield strength f_y .

References

- Ahmed, M., Oehlers, D.J. and Bradford, M.A. (2000), "Retrofitting reinforced concrete beams by bolting steel plates to their sides. Part 1: Behavior and experiments", *Struct. Eng. Mech., Int. J.*, **10(3)**, 211-226.
- Brian Uy, and Andrew Bradford (1995), "Ductility of Profile Beams. Part : Experimental Study", *ASCE J. Struct. Eng.*, **121(5)**, 876-882.
- Brian Uy, and Andrew Bradford (1995), "Ductility of Profile Beams. Part : Analytical Study", *ASCE J. Struct. Eng.*, **121(5)**, 883-889.
- Hyung-Joon Ahn, Soo-Hyun Ryu (2007), "Experimental Study on Flexural Strength of Modular Composite Profile Beams" *Steel Compo. Struct. An Int. J.*, **7(1)**, 71-85.
- Minglan Peng and Zhifei Shi (2004), "Interface characteristics of RC beams strengthened with FRP plate" *Struct. Eng. and Mech., An Int. J.*, **18(3)**, 315-330.
- Oehlers D.J. (1993), "Composite Profile Beams" *ASCE J. Struct. Eng.*, **119(4)**, 1085-1100.
- Oehlers D.J., Wright H.D. and Burnet M.J. (1994), "Flexural Strength of Profile Beams", *ASCE J. Struct. Eng.*, **120(2)**, 378-393.
- Oehlers, D.J., Ahmed, M., Nguyen N.T. and Bradford, M.A. (1997), "Transverse and Longitudinal partial interaction in composite bolted side-plated reinforced concrete beams", *Struct. Eng. Mech., An Int. J.*, **5(5)**, 553-563.
- Oehlers, D.J., Ninh T Nguyen and Bradford, M.A. (2000), "Retrofitting by adhesive bonding steel plates to sides of R.C. beams. Part 1: Debonding of plates due to flexure, *Struct. Eng. Mech., An Int. J.*, **9(5)**, 491-503.
- Oehlers, D.J., Ninh T Nguyen and Bradford, M.A. (2000), "Retrofitting by adhesive bonding steel plates to sides of R.C. beams. Part 2: Debonding of plates due to shear and design rules", *Struct. Eng. Mech., An Int. J.*, **9(5)**, 505-518.
- Oehlers, D.J., Ahmed, M., Nguyen N.T. and Bradford, M.A. (2000), "Retrofitting reinforced concrete beams by bolting steel plates to their sides. Part 2: Transverse interaction and rigid plastic design", *Struct. Eng. Mech., An Int. J.*, **10(3)**, 227-243.
- Sang Hun Kim and Riyad S. Aboutaha, (2004), "Ductility of carbon fiber-reinforced polymer (CFRP) strengthened reinforced concrete beams: Experimental investigation" *Steel Compo. Struct. An Int. J.*, **4(5)**.